

# Radio frequency excited waveguide CO<sub>2</sub> lasers on sequence-band transitions

S.-Y. Shaw, R.-S. Chang

Department of Electrical Engineering, National Tsing Hua University, Hsinchu, Taiwan 30043, R.O. China  
 (Fax: +886-3/5715971, E-mail: sysh@ee.nthu.edu.tw)

Received: 29 September 1997/Revised version: 2 December 1997

**Abstract.** Radio frequency (RF) excited waveguide CO<sub>2</sub> lasers based on either a quartz or an alumina waveguide were studied on the 00°2 - [10°1, 02°1]<sub>I,II</sub> sequence bands. A compact multisegment RF excitation with capacitive coupling was used for pumping the gain section of the laser waveguide. The use of a separate intracavity hot CO<sub>2</sub> waveguide suppresses the regular-band transitions. The quartz waveguide laser has a total of 62 lines lasing on both the 9.4 and 10.4 μm sequence bands. The alumina waveguide laser has 40 lines lasing on the 10.4 μm sequence band. These lasers can be either pulsed or continuous-wave (CW) operated on the selected line without a line jumping problem.

**PACS:** 42.55.Dk; 42.60.By; 42.72.+h

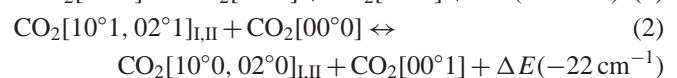
Since the first report by Reid and Siemsen [1, 2] of laser emission on the 00°2 - [10°1, 02°1]<sub>I,II</sub> sequence bands, where I and II respectively denote the 9.4 μm and 10.4 μm transitions terminating the mixing of (10°1) and (02°1) states, a great deal of research has been carried out with various approaches. Solodukhin [3] used a non-Littrow mounted grating in a hot-cell-free cavity. Kikhlevskiv et al. [4] employed an interference filter in a CO<sub>2</sub> waveguide laser cavity and achieved a single line sequence-band output. Evenson et al. [5] obtained several sequence-band and hot-band lines using a simple cavity tuned by a 171 groove/mm grating. Compared with the use of an optical cavity with very high wavelength discrimination, the utilization of an intracavity hot CO<sub>2</sub> cell is a simple and efficient method of suppressing the regular-band transitions [6]. The intracavity hot cell has been successfully applied in conventional low-pressure lasers [2] and transversely excited atmospheric-pressure (TEA) lasers [7, 8] to achieve sequence-band oscillation. In [9, 10], we described dc-discharged waveguide CO<sub>2</sub> lasers with an intracavity hot cell that yielded line tunable sequence-band output.

The sequence bands provide a considerably increased number of CO<sub>2</sub> laser lines for applications such as optical pumping of far infrared (FIR) lasers [11, 12] and laser spectroscopy of molecules [13], where a maximized wavelength coverage of the light source is preferred. In addition, it can be

used for studies involving propagation of laser beams through the atmosphere. Owing to its wide tuning range, the waveguide CO<sub>2</sub> lasers operated in the regular bands have been used by different groups [14–17] for pumping FIR lasers and laser spectroscopy. For all these applications, a compact and reliable sequence-band waveguide CO<sub>2</sub> laser would be highly preferable. In the past decade, the RF excitation techniques have been successfully developed for the pumping of waveguide CO<sub>2</sub> lasers [18–20]. The advantages of low-voltage operation, electrodeless construction, uniform α-discharge and easiness of discharge switching introduced by the RF excitation, lead to the possibility of a very compact and user-friendly high-power waveguide CO<sub>2</sub> laser. In [21] we described the preliminary results on the sequence-band oscillation in an RF-excited waveguide CO<sub>2</sub> laser. In this paper we will report the design and performance of RF excited waveguide CO<sub>2</sub> lasers which are able to lase on most lines in the 00°2 - [10°1, 02°1]<sub>I,II</sub> sequence bands.

## 1 Oscillation on sequence bands

The transition dynamics of the CO<sub>2</sub> laser under a gas discharge have been studied in detail for years. The mode-temperatures model introduced by Moore et al. [22] and Gordietz et al. [23], which separately characterizes the vibrational temperatures of the three vibrational modes of the CO<sub>2</sub> molecule, has been successfully applied to the description of both CW and pulsed CO<sub>2</sub> lasers. Due to the strong coupling by collisions in the discharge of a CO<sub>2</sub>-N<sub>2</sub>-He gas mixture, the vibrational levels [00°*n*], *n* ≤ 4, are in equilibrium with each other in less than 10 μs under laser conditions [24]. The excitation and relaxation processes for the laser levels of sequence bands with *n* = 2 involve the collisional energy transfer between CO<sub>2</sub> molecules given by



The relaxation process (2) is very fast, of the order of  $4 \times 10^6 / \text{Torr s}$  [25, 26]. It is followed by the relaxation of the low-lying levels  $[10^0, 02^0]_{I,II}$  of regular bands.

In terms of the mode temperatures, the population of the vibrational levels is Boltzmann distributed and the gain ratio of corresponding lines of the sequence and regular bands may be given by

$$(\gamma_{\text{seq}}/\gamma_{\text{reg}}) = (\mu_{\text{seq}}/\mu_{\text{reg}})^2 \exp(-h\nu_3/kT_3) \quad (3)$$

where  $\gamma$  is the gain coefficient,  $\mu$  is the matrix element of the electric dipole transition,  $T_3$  is the mode temperature associated with the asymmetric stretch vibration  $\nu_3$ . The subscripts seq and reg refer to sequence and regular bands, respectively. In the literature [27, 28], the ratio  $(\mu_{\text{seq}}/\mu_{\text{reg}})^2$  is found to be 1.89 for the  $9.4 \mu\text{m}$  band and 2.1 for the  $10.4 \mu\text{m}$  band. For a system lasing in regular bands [29],  $T_3$  is about 1000 K and the gain ratio is only  $\cong 0.13$ . When the vibrational temperature  $T_3$ , is about 2000 K, as indicated in a discharge with lower  $\text{CO}_2$  content [28], a gain ratio  $\approx 0.4$  can be achieved. Since all transitions are collisionally coupled, strong competition between all potential laser lines determines the laser oscillation. A laser cavity for sequence-band lasing must provide small cavity losses on the sequence lines and much larger losses on the regular lines.

In the case of a waveguide  $\text{CO}_2$  laser resonator composed of a gain section and a hot  $\text{CO}_2$  absorption section, the conditions for suppressing the regular bands and lasing of sequence bands are given by

$$\gamma_{\text{reg}} l_{\text{gain}} - \alpha_{\text{reg}} l_{\text{cell}} - T - L_W - L_C < 0, \quad (4)$$

$$\gamma_{\text{seq}} l_{\text{gain}} - T - L_W - L_C > 0, \quad (5)$$

where  $l_{\text{gain}}$  and  $l_{\text{cell}}$  are the lengths of gain and absorption sections, respectively;  $\alpha_{\text{reg}}$  is the absorption coefficient of the regular line in the absorption section;  $T$  is the transmittance of the output coupler;  $L_W$  is the guiding loss of the waveguide, and  $L_C$  is the coupling loss at the ends of the waveguide. For a given  $\alpha_{\text{reg}}$ , the length  $l_{\text{cell}}$  can be arbitrarily increased to satisfy (4). However, a larger  $l_{\text{cell}}$  results in a higher guiding loss  $L_W$ , which may hinder the oscillation of sequence bands due to the relatively small gain coefficient  $\gamma_{\text{seq}}$ . Thus a minimum length of absorption section should be established from the parameters associated with the corresponding sequence line.

## 2 Experimental

The experimental study was based on an RF excited flowing-gas  $\text{CO}_2$  waveguide laser similar to that described in [30]. We have experimented with waveguides of either quartz or 99.5% alumina ceramic. Both waveguides had an inner diameter of 3 mm and wall thickness of 1 mm. The alumina waveguide was an ordinary protection tube for thermocouples used in high temperature applications. No additional polishing of its inner surface was attempted. The quartz waveguide was a precision-bore tubing with a very fine inner surface.

The laser configuration is shown schematically in Fig. 1. Eight pairs of water-cooled aluminum electrodes 10 cm long were clamped oppositely onto the outer surface of the discharge waveguide. A proper amount of thermally conductive paste was glued between the electrodes and waveguide for better cooling of the discharge region. Each pair of electrodes was driven by an individual RF power module through an impedance matching circuit. Proper electrical shielding between each electrode pair was installed to prevent undesired coupling between adjacent electrodes, which could result in non-uniform discharge due to the formation of standing waves along the electrodes, normally observed in high-frequency transmission lines [31]. The impedance matching circuit was a high-Q  $L_1 - L - C_2$   $\pi$ -network with strip-line inductance, which has been used for efficient excitation of waveguide  $\text{CO}_2$  lasers [30]. The utilization of segmented RF excitation leads to several advantages. The impedance matching of each discharge segment can be individually optimized to yield nearly perfect power transfer to the discharge and a better uniformity of RF  $\alpha$  discharge along the waveguide. The use of a low power RF module instead of a single high power RF generator, which has been used by most authors, greatly improves system reliability whilst reducing cost since high quality RF components for high power circuits are usually very expensive.

The discharge section was operated with a flowing gas mixture symmetrically injected and pumped out via the two ends and the inlet and outlet holes on the discharge waveguide, as shown in Fig. 1. One end of the discharge waveguide was sealed by a gold-coated flat mirror mounted on a piezoelectric (PZT) actuator for cavity length tuning. The distance between mirror and waveguide was 2 mm, so a Case I coupling was formed. The other end of the dis-

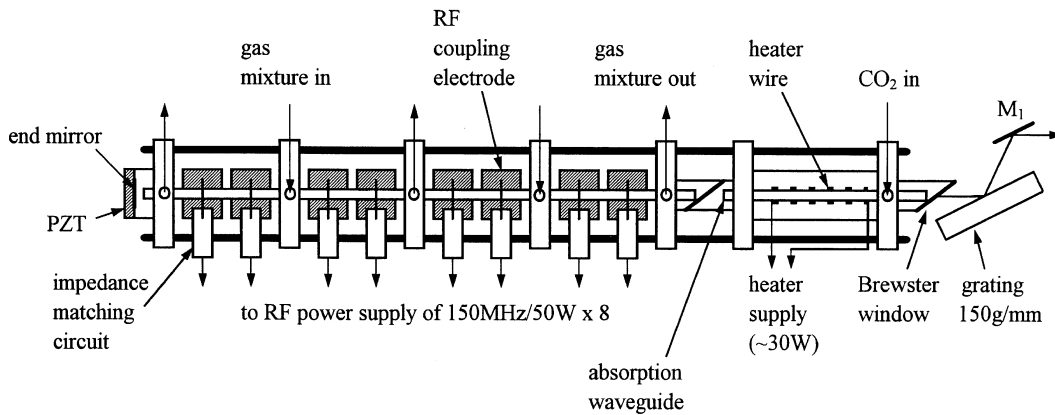


Fig. 1. Schematic drawing of the RF-excited sequence-band waveguide  $\text{CO}_2$  laser

charge waveguide was followed by the absorption waveguide. A ZnSe Brewster window of 2 mm thickness served as vacuum-tight sealing between the discharge and absorption waveguides, so that the gas contents of both waveguide sections could be individually varied. The mounting of the absorption waveguide was designed to enable precise adjustment for optical alignment. The smallest distance, about 8 mm, between the two waveguide ends was chosen to minimize coupling loss. The output end of the absorption waveguide was sealed by a ZnSe Brewster window. A stainless steel grating of 150 groove/mm blazed at  $10.6 \mu\text{m}$  wavelength (made by Hyperfine, Inc.) was placed at a distance of  $\sim 2.5 \text{ cm}$  from the Brewster window. The grating was mounted at Littrow orientation and the laser beam was coupled out through the zero order diffraction, which provided around 5% output coupling from 9–11  $\mu\text{m}$ . A precision rotation stage controlled the grating for wavelength tuning and the beam steering reflector  $M_1$  moved synchronously to keep the direction of the output beam unchanged during wavelength tuning.

The absorption waveguide was heated by a heater wire wound around the waveguide. A larger Pyrex tube outside the waveguide provided heat insulation. Electrical power of  $\sim 30 \text{ W}$  applied to the heater wire produced a temperature of  $\sim 350 \text{ }^\circ\text{C}$  in the waveguide. The absorption waveguide was filled with pure  $\text{CO}_2$  gas at a pressure equal to the total gas pressure in the discharge waveguide. The effective length of the absorption waveguide was determined, from (4) and (5), to be  $\approx 20 \text{ cm}$  using estimated values of  $\gamma_{\text{reg}} \sim 1\% \text{ cm}^{-1}$ ,  $\gamma_{\text{seq}} \sim 0.4\% \text{ cm}^{-1}$ ,  $T \sim 5\%$ ,  $\alpha_{\text{reg}} \sim 3\% \text{ cm}^{-1}$ ,  $L_W \sim 3\%$  and  $L_C \sim 15\%$ . The total length of our optical cavity was  $\cong 125 \text{ cm}$ .

The laser gain medium was typically a gas mixture of  $\text{CO}_2 : \text{N}_2 : \text{He} = 1 : 2 : 7$  at a flow rate of about 2 SCFH (standard cubic foot per hour) and pressure of about 60 Torr. No special effort was made to optimize the gas composition. Each discharge segment was driven by an RF power of about 50 W at 150 MHz frequency. For all the measurements in this

experiment, each impedance matching circuit was adjusted to have a standing wave ratio (SWR)  $\leq 1.5$ . Due to the advantage of RF excitation, the discharge can be stably operated in pulsed mode with a repetition rate of up to 100 Hz. In this experiment, the RF power modules were pulse modulated at a repetition of 10 Hz and adjustable duty factor between 10% and 100%.

The laser output power was monitored using a thermopile power meter. The laser spectral signature was observed by a  $\text{CO}_2$  laser spectrum analyzer. Most of the sequence lines appeared midway between the two adjacent regular lines. An obvious shift on the panoramic screen of the spectrum analyzer can be observed when the hot  $\text{CO}_2$  cell took effect, resulting in the change of lasing from the regular lines to the sequence lines. The lasing of the sequence lines was also identified by detecting the  $4.3 \mu\text{m}$  fluorescence signal in an external low pressure  $\text{CO}_2$  cell [32]. The fluorescence was easily produced when the laser of regular lines passed through the  $\text{CO}_2$  cell. But there was no fluorescence from the sequence lines because the population of  $[10^0 1, 02^0 1]_{\text{I,II}}$  levels for producing the fluorescence is relatively low in a room temperature  $\text{CO}_2$  cell.

In our experiments, we changed the RF power, the duty factor of the pulsed discharge, the cooling water temperature and gas pressure to study their effects on the laser output power. The results will be summarized in the next section.

### 3 Experimental results

#### 3.1 Laser output power

The laser peak power for the quartz waveguide laser, as determined from the measured laser average power and the pulse duty factor, are indicated in Fig. 2 and 3. These results were obtained at a pressure of 60 Torr, an RF peak power of 50 W per discharge segment with a 50% duty factor at 10 Hz repetition rate and cooling water temperature of  $10 \text{ }^\circ\text{C}$ . We recorded

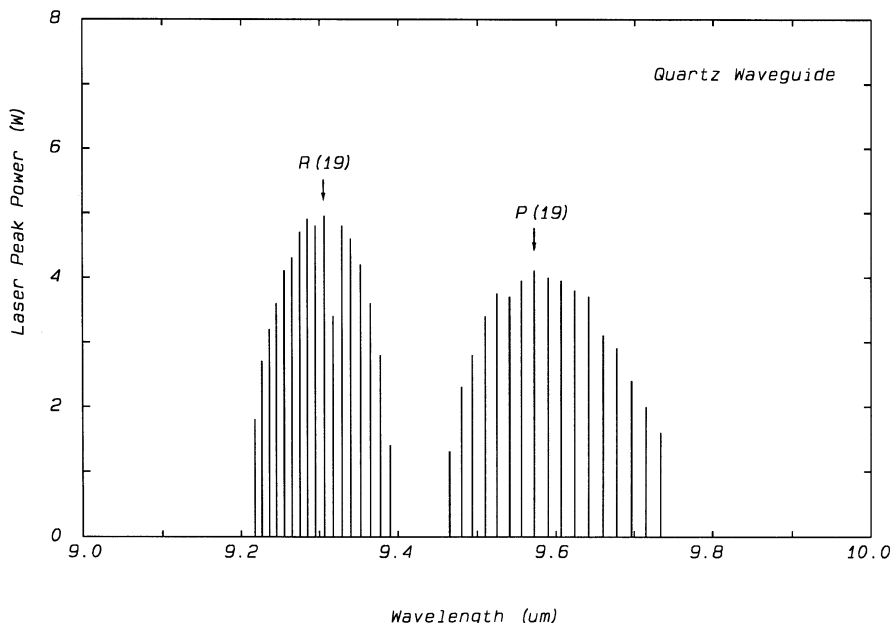


**Fig. 2.** Laser peak power of the  $9.4 \mu\text{m}$  sequence band observed in the quartz waveguide laser for 60 Torr of  $\text{CO}_2 : \text{N}_2 : \text{He} = 1 : 2 : 7$  discharged at 50% RF excitation duty factor

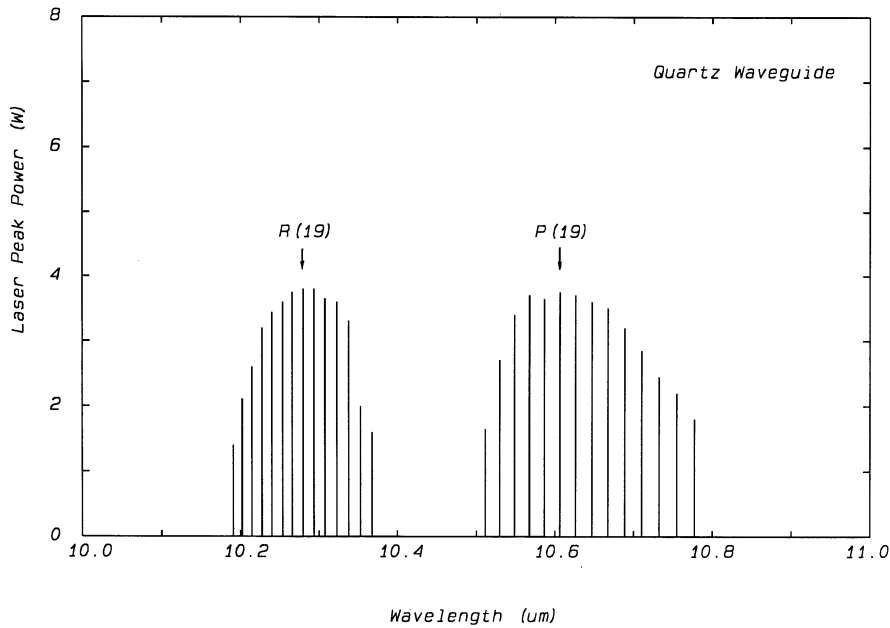


**Fig. 3.** Laser peak power of the 10.4  $\mu\text{m}$  sequence band observed in the quartz waveguide laser for 60 Torr of  $\text{CO}_2 : \text{N}_2 : \text{He} = 1 : 2 : 7$  discharged at 50% RF excitation duty factor

a total of 62 lines in the sequence bands, 34 lines in the 9.4  $\mu\text{m}$  band and 28 lines in the 10.4  $\mu\text{m}$  band. The maximum peak power was 5 W. We found that the strongest line in each branch of the sequence bands had more than 45% of the power of the corresponding regular line under the same conditions.

For the alumina waveguide laser we obtained 40 lines in the 10.4  $\mu\text{m}$  sequence band. The results are shown in Fig. 4. It was difficult to obtain oscillation on the 9.4  $\mu\text{m}$  sequence band. Nevertheless, the output power and the number of lines on the 10.4  $\mu\text{m}$  sequence band were superior to the quartz waveguide laser. The strongest line had a peak power of 6.5 W, which is about 60% of that for the corresponding regular line.

### 3.2 Effects of cooling water temperature and pulsed discharge duty factor

At a gas pressure of 60 Torr we varied the cooling water temperature and the discharge duty factor to study their effects. Figures 5 and 6 show the results of the sequence line 10SP(19) and the regular line 10P(20) for comparison. In the quartz waveguide laser the laser peak power decreased by about 10% for the sequence line when the cooling water temperature increased from 10  $^{\circ}\text{C}$  to 18  $^{\circ}\text{C}$ , whereas the regular line decreased by the same amount at 32  $^{\circ}\text{C}$ . When the duty factor increased from 10% to 100%, the laser average power of the sequence line began to decline at 55% duty factor, whereas the regular line maintained a linear increase up to

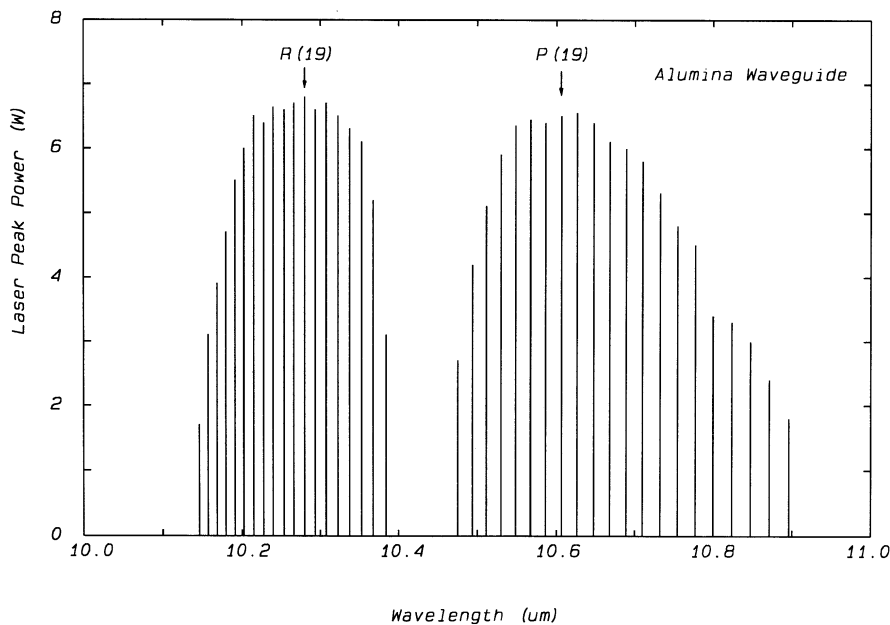


**Fig. 4.** Laser peak power of the 10.4  $\mu\text{m}$  sequence band observed in the alumina waveguide laser for 60 Torr of  $\text{CO}_2 : \text{N}_2 : \text{He} = 1 : 2 : 7$  discharged at 50% RF excitation duty factor

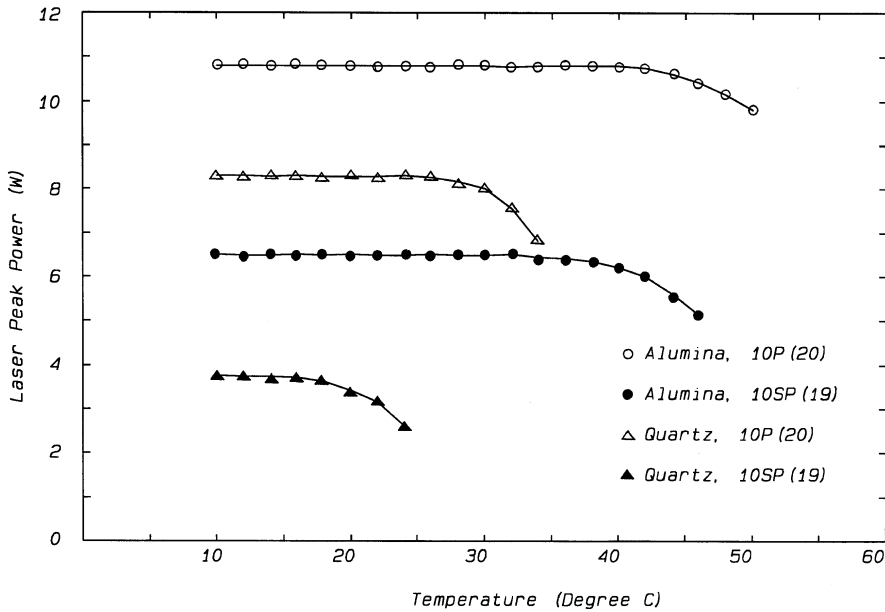


**Fig. 5.** Laser peak power of sequence and regular lines versus cooling water temperature for 60 Torr of  $\text{CO}_2 : \text{N}_2 : \text{He} = 1 : 2 : 7$  discharge with 50% RF excitation duty factor at the peak power of 50 W/segment

70% duty factor. In the alumina waveguide laser, the output power began to decrease when the cooling water temperature reached 35 °C and 42 °C for sequence and regular lines, respectively. The laser average power maintained a linear increase up to 100% duty factor for both sequence and regular lines.

### 3.3 Effects of gas pressure and RF power

The gas pressure and RF power were varied in a small range to study the resulting effects. Figure 7 shows the results for the 10SP(19) sequence line in the quartz waveguide laser. When the RF peak power was 40 W for each discharge segment at 50% duty factor, a stable discharge was found for the pressure below 50 Torr. When the RF power increased to

50 W, the gas pressure could be operated up to 70 Torr. The laser power for both sequence and regular lines began to decrease when the pressure exceeded 60 Torr.

### 3.4 Frequency tunability

The laser power was measured as a function of cavity length to determine the frequency tuning range. We found that the tuning range for the strong sequence lines was limited by the free spectral range (FSR) of the cavity. In our lasers the FSR was  $\approx 120$  MHz for the cavity length of  $\approx 125$  cm. The pressure broadening of the gain curves was around 200–300 MHz when the laser was operated at a gas pressure of 40–60 Torr. We observed that a frequency scan without longitudinal mode hopping could be attained over the FSR.

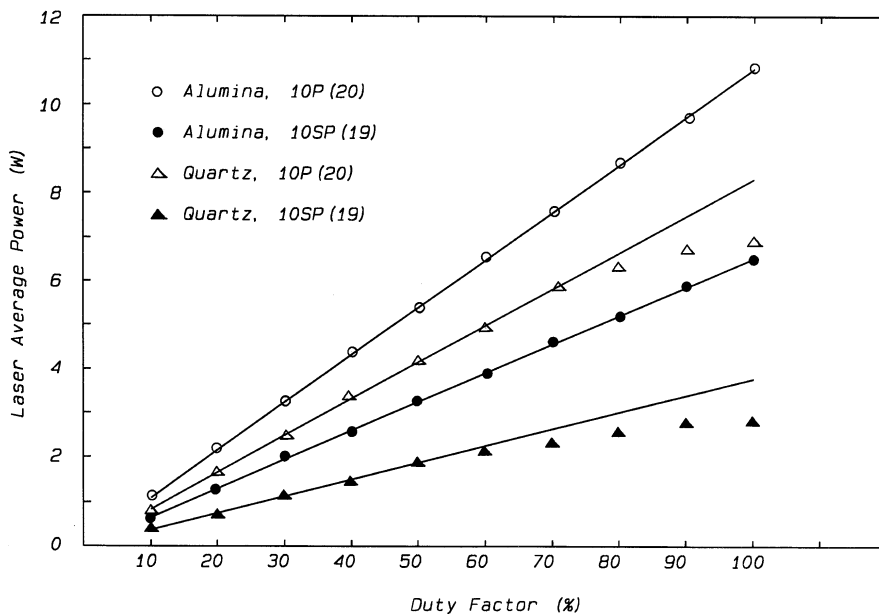


**Fig. 6.** Laser average power of sequence and regular lines versus duty factor for 60 Torr of  $\text{CO}_2 : \text{N}_2 : \text{He} = 1 : 2 : 7$  discharge with cooling water temperature of 10 °C and RF peak power of 50 W/segment

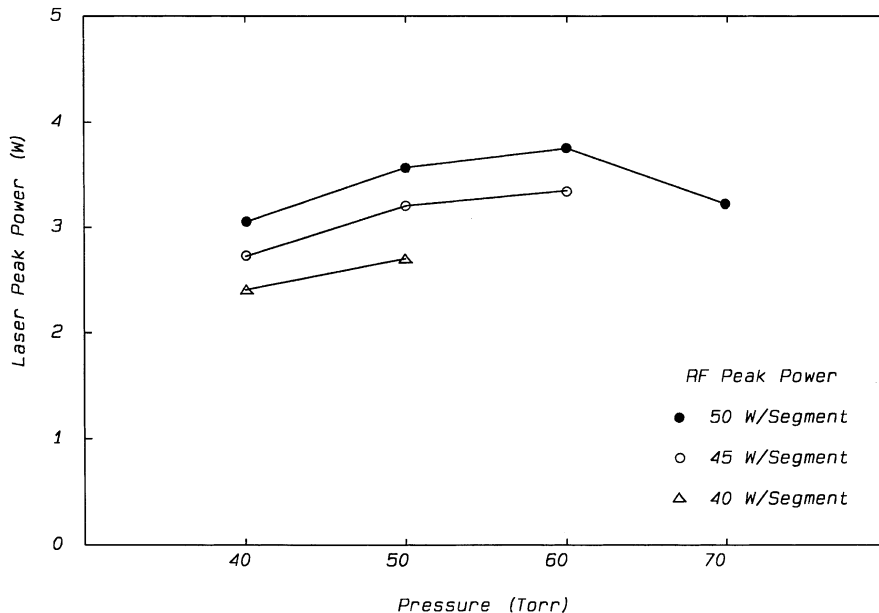


Fig. 7. Laser peak power of sequence line versus gas pressure and RF peak power with cooling water temperature of 10 °C and 50% duty factor

The wavelength discrimination of a grating-tuned laser cavity is determined by the spectral resolution and illumination area of the grating. A waveguide laser usually combines a beam expander at the grating to achieve sufficient line selectivity. In our simple waveguide laser resonator we found that the use of 150 groove/mm grating could yield single-line operation over the sequence band transitions.

#### 4 Discussion and conclusions

Using the quartz waveguide laser, we obtained a total of 62 sequence lines. Most of the lines had more than 1 W output peak power. We studied the effects of RF excitation power, gas pressure, cooling water temperature and duty factor of pulsed discharge for a gas mixture with low CO<sub>2</sub> content. The low CO<sub>2</sub> content in the gas mixture leads to the higher value of  $T_3$  in the dc discharge of this gas mixture [28, 33], and consequently favors the sequence band oscillation [10]. The results of this experiment suggest that the gas mixture used in dc discharged sequence band lasers works well for RF excited systems. The optimum gas pressure of our laser was about 60 Torr. The increased gas pressure resulted in higher gas temperature and faster collisional de-excitation of the  $\nu_3$  mode which could reduce the gain coefficient [28]. The optimum conditions for the sequence bands will be studied by gain coefficient and saturation intensity measurements in a waveguide laser amplifier. The dependence of laser peak power on the cooling water temperature and discharge duty factor revealed that the cooling of the discharge region became marginal at 55% duty factor. Improved facilities for cooling the discharge waveguide would be required to achieve CW operation, if necessary, in the quartz waveguide laser.

In the alumina waveguide laser under the same conditions, better performance in the 10.4  $\mu\text{m}$  sequence band was obtained compared with the quartz waveguide laser. A total of 40 sequence lines were found, and almost twice the laser power of the quartz waveguide laser was observed. Since the thermal conductivity of alumina is a factor 20 higher than that

of quartz, the cooling effect should be much better for the alumina waveguide. It is a reasonable consequence of a higher optical gain in the discharge of the alumina waveguide. However, it was difficult to achieve lasing on the 9.4  $\mu\text{m}$  sequence band. As this was also observed in [10, 34, 35], the behavior may be explained by the dispersion property of the alumina waveguide: guiding of optical waves changes at  $\sim 10 \mu\text{m}$  from being leaky at shorter wavelengths to being attenuated by total internal reflection at longer wavelengths.

Finally, the use of pulsed RF excitation at a repetition rate of 10 Hz and duty factor over 10% yielded a steady state oscillation for lines of both sequence and regular bands. As observed using a fast HgCdTe detector, the shape of the laser pulses was rectangular with a nearly flat top at the period of excitation. Since the build-up time for oscillation in a CO<sub>2</sub> laser is of the order of microseconds, no transient effect was recorded in our laser. By tuning and selecting the sequence lines carefully with the 150 groove/mm grating, we did not have a line jumping problem with our lasers.

In conclusion, the sequence band CO<sub>2</sub> waveguide lasers we have described can provide a single line and wide tuning range with relatively high peak power. The installation of a segmented RF discharge and a gas-isolated absorption CO<sub>2</sub> cell resulted in compact systems with user-friendly operation. These lasers can be a useful source for pumping FIR lasers and laser spectroscopic studies.

*Acknowledgements.* This work was supported by the National Science Council of the Republic of China under contract NSC-85-2215-E-007-002.

#### References

1. J. Reid, K.J. Siemsen: *Appl. Phys. Lett.* **29**, 250 (1976)
2. J. Reid, K.J. Siemsen: *J. Appl. Phys.* **48**, 2712 (1977)
3. A.S. Solodukhin: *J. Mod. Opt.* **34**, 577 (1987)
4. S.V. Kukhlevskil, A.S. Provorov, M.Yu. Reushev: *Sov. J. Quantum Electron.* **19**, 308 (1989)
5. K.M. Evenson, C.C. Chou, B.W. Bach, K.G. Bach: *IEEE J. Quantum Electron.* **30**, 1187 (1994)

6. W. Berger, K.J. Siemsen, J. Reid: *Rev. Sci. Instrum.* **48**, 1031 (1977)
7. R.K. Brimacombe, J. Reid, T.A. Znotins: *Appl. Phys. Lett.* **39**, 302 (1981)
8. I.M. Bertel', V.O. Petukhov, S.A. Trushin, V.V. Churakov: *Sov. J. Quantum Electron.* **11**, 213 (1981)
9. T.K. Ho, S.Y. Shaw, J.T. Shy: *J. Appl. Phys.* **74**, 6460 (1993)
10. T.K. Ho, S.Y. Shaw, J.T. Shy: *Appl. Phys. B* **61**, 95 (1995)
11. C.O. Weiss, M. Grinda, K.J. Siemsen: *IEEE J. Quantum Electron.* **13**, 892 (1977)
12. M. Redon, C. Gastaud, M. Fourier: *Opt. Lett.* **9**, 71 (1984)
13. J.W.R. Tabosa, R.R. Leite: *Opt. Lett.* **10**, 544 (1985)
14. N. Ioli, G. Moruzzi, F. Strumia: *Nuovo Cimento* **28**, 257 (1980)
15. G. Merkle, J. Heppner: *Opt. Commun.* **51** 165 (1984)
16. F. Tang, J.O. Henningsen: *IEEE J. Quantum Electron.* **22**, 2084 (1986)
17. E.M. Telles, J.G.S. Moraes, A. Scalabrin, D. Pereira, G. Carelli, N. Ioli, A. Moretti, F. Strumia: *IEEE J. Quantum Electron.* **30**, 2946 (1994)
18. D. He, D.R. Hall: *Appl. Phys. Lett.* **43**, 726 (1983)
19. D.R. Hall: In *Handbook of Molecular Lasers*, ed. by P.K. Cheo (Dekker, New York 1987) Chap. 3
20. M. Khelkhal, F. Herlemont: *IEEE J. Quantum Electron.* **29**, 818 (1993)
21. S.Y. Shaw: Conference on Laser and Electro-Optics, CLEO'96, CA, USA, in *Technical Digest* (1996) pp. 444
22. C.B. Moore, R.E. Wood, B.E. Hu, J.T. Yardley: *J. Chem. Phys.* **46**, 4222 (1967)
23. B.F. Gordietz, N.N. Sobolev, V.V. Sokovikov, L.A. Shelepin: *IEEE J. Quantum Electron.* **4** 796 (1968)
24. L.O. Hocker, M.A. Kovacs, C.K. Rhodes, G.W. Flynn, A. Javan: *Phys. Rev. Lett.* **17**, 233 (1966)
25. J. Finzi, C.B. Moore: *J. Chem. Phys.* **63**, 2285 (1975)
26. R.T. Pack: *J. Chem. Phys.* **72**, 6140 (1980)
27. J. Reid, J. Shewchun, B.K. Garside: *Appl. Phys.* **17**, 349 (1978)
28. K.J. Siemsen, J. Reid, C. Dang: *IEEE J. Quantum Electron.* **16**, 668 (1980)
29. C. Dang, J. Reid, B.K. Garside: *IEEE J. Quantum Electron.* **19**, 755 (1983)
30. S.Y. Shaw, R.S. Chang: *Proc. Natl. Sci. Counc. ROC(A)* **21**, 623 (1997)
31. R.L. Sinclair, J. Tulip: *J. Appl. Phys.* **56**, 2497 (1984)
32. C. Freed, A. Javan: *Appl. Phys. Lett.* **17**, 53 (1970)
33. J. Mellis, A.L.S. Smith: *Opt. Commun.* **41**, 121 (1982)
34. R.M. Jenkins, R.W.J. Devereux: *IEEE J. Quantum Electron.* **21**, 1722 (1985)
35. S.J. Saggese, J.A. Harrington, G.H. Sigel, Jr., R. Altkorn, R. Haidle: *Appl. Spectrosc.* **46**, 1194 (1992)